Evidence for impaired hydrogen-bonding of tyrosine Y_Z in calcium-depleted Photosystem II

Michael Haumann, Wolfgang Junge *

Abteilung Biophysik, Fachbereich Biologie/Chemie, Universität Osnabrück, D-49069 Osnabrück, Germany

Abstract

Photosystem II (PS II) evolves oxygen from two bound water molecules in a four-stepped reaction that is driven by four quanta of light, each oxidizing the chlorophyll moiety P_{680} to yield P_{680}^+. When starting from its dark equilibrium (mainly state S_1), the catalytic center can be clocked through its redox states ($S_0...S_4$) by a series of short flashes of light. The center involves at least a Mn_4-cluster and a special tyrosine residue, named Y_Z, as redox cofactors plus two essential ionic cofactors, Cl^- and Ca^{2+}. Centers which have lost Ca^{2+} do not evolve oxygen. We investigated the stepped progression in dark-adapted PS II core particles after the removal of Ca^{2+}. Y_Z was oxidized from the first flash on. The difference spectrum of $Y_Z \rightarrow Y_Z^{ox}$ differed from the one in competent centers, where it has been ascribed to a hydrogen-bonded tyrosinate. The rate of the electron transfer from Y_Z to P_{680}^+ was slowed down by three orders of magnitude and its kinetic isotope effect rose up from 1.1 to 2.5. Proton release into the bulk was now a prerequisite for the electron transfer from Y_Z to P_{680}^+. On the basis of these results and similar effects in Mn-(plus Ca^{2+}-)depleted PS II (M. Haumann et al., Biochemistry, 38 (1999) 1258–1267) we conclude that the presence of Ca^{2+} in the catalytic center is required to tune the apparent pK of a base cluster, B, to which Y_Z is linked by hydrogen bonds. The deposition of a proton on B within close proximity of Y_Z (not its release into the bulk!) is a necessary condition for the reduction in nanoseconds of P_{680}^+ and for the functioning of water oxidation. The removal of Ca^{2+} rises the pK of B, thereby disturbing the hydrogen bonded structure of Y_ZB. © 1999 Elsevier Science B.V. All rights reserved.

Keywords: Photosystem II; Water oxidation; Tyrosine$_Z$; Hydrogen bonding; Calcium depletion

1. Introduction

Photosystem II (PS II) evolves oxygen from two bound water molecules at a site that contains at least a manganese cluster, Mn_4, and a special tyrosine residue (D_1Tyr161), named Y_Z, as redox cofactors plus one atom of each Ca^{2+} and Cl^- (see [1] for review). The presence of a further cofactor (X) is under debate (see [2,3] and references therein). Each absorbed quantum of light induces a primary electron transfer from the chlorophyll *a*-moiety P_{680}, to the primary quinone acceptor Q_A. P_{680}^+ is reduced

by Mn_4X via the tyrosine, Y_Z [4]. These cofactors are located at the lumenal site of PS II and they are probably bound to the D_1 subunit. According to current structural models of PS II, it is likely that they are located at about the same depth in the membrane [5] and within a small area of about 15×15 Å [6–8]. PS II can be depleted from Mn, Ca^{2+} and Cl^- without complete loss of the *photochemical* activity [1]. Oxygen evolution, however, is inhibited by each of these treatments, and the midpoint potentials of the redox cofactors are altered. In the absence of Ca^{2+}, Mn_4XY_Z has been reported to be oxidizable only twice [9,10]. Thereafter, the rapid recombination of the charge pair $P_{680}^+Q_A^-$ occurs. In Ca^{2+}-depleted material the reduction of P_{680}^+ by Y_Z is retarded by orders of magnitude [11,12]. Even the midpoint potential of Q_A at the other side of the membrane is increased [13]. Despite of these drastic effects of Ca^{2+} depletion, information on the properties of Y_Z in Ca^{2+}-depleted PS II, as gained by magnetic resonance techniques, has been claimed to represent the properties of Y_Z in the functional, i.e., oxygen-evolving system. On this basis, rather specific models for the chemical mechanism of water oxidation have been postulated wherein Y_Z^{ox} is considered as a hydrogen acceptor from bound water [14,15].

Our previous laser-flash spectrophotometric studies with Mn-depleted PS II versus intact PS II have led to the suggestion that Y_Z may be present as a tyrosine in the former case but as a hydrogen-bonded tyrosinate in active centers. Only in Mn-depleted centers and at acid pH [16,17] does the oxidation of Y_Z cause the release of a proton into the bulk. There is evidence, in oxygen-evolving PS II [18,19] and also in dysfunctional centers under certain conditions [20–23], that the phenolic proton may stay close to Y_Z even after its oxidation. It is probably shared with an acid/base-cluster, B. The capturing of the phenolic proton within the protein and close to Y_Z^{ox} is difficult to reconcile with the proposed hydrogen acceptor function of Y_Z^{ox}.

The removal of Mn which also removes Ca^{2+} is a rather drastic inactivation of the catalytic center. It is only reversible by a complicated protocol involving the light induced oxidation of added Mn^{II} [1]. The removal of Ca^{2+} is another way to inactivate the catalytic center, but it is readily reversible even in the dark. In this work we investigated the effects of

Ca^{2+} depletion on the properties of Y_Z. We found drastic effects on the difference spectrum of $Y_Z \rightarrow Y_Z^{ox}$, on electric charge transients, on proton release, on the rate of the electron transfer between Y_Z and P_{680}^+ and on its kinetic isotope effect. This behavior resembled the one observed in Mn-depleted PS II at acid pH. Some of these effects are probably owed to the concomitant loss of Ca^{2+} in Mn-depleted material. It appears as if Ca^{2+} is required to tune the pK of the acid/base-cluster in contact with Y_Z in a way as to install the proper hydrogen-bonded structure for rapid electron transfer from Y_Z to P_{680}^+.

2. Materials and methods

Oxygen-evolving PS II core particles were prepared from pea seedlings according to [24]. They lack the 17 and 23 kDa extrinsic proteins [25].

Ca^{2+} depletion was achieved by a modified low pH/citrate-treatment [26] which is known to extract Ca^{2+} in darkness from all S-states without concomitant extraction of Mn [27]. After thawing, particles were washed at ~ 10 μM of chlorophyll in 20 mM NaCl, 10 mM BisTris (pH 6), recollected by centrifugation (1 h, 3°C, $100\,000 \times g$), and suspended at ~ 1 mM chlorophyll in 20 mM NaCl, 0.03% w/v βDM, and 10 mM BisTris, pH 6.5. Before the measurements particles were diluted to ~ 30–150 μM chlorophyll in 10 mM citrate (pH 3.5), 20 mM NaCl and 0.03% βDM, and gently stirred for 3 min on ice in the dark. After this, 20 mM BisTris (pH 6.5) or tricine (pH 7.5), 20 mM NaCl and 0.03% βDM were added up to a final chlorophyll concentration of 8 μM. EDTA (1 mM) was added, if necessary, after the citrate treatment, before the buffers. All treatments were carried out in darkness. Oxygen evolution under continuous light (Clark-type electrode, 500 μM DCBQ, 1 mM hexacyanoferrate(III)) was $\sim 10\%$ of a non-treated control (~ 1200 μmol O_2/mg chl h) in the Ca^{2+}-depleted PS II.

Ca^{2+} repletion was achieved by the addition of 20 mM of $CaCl_2$. Oxygen evolution was about 80% of an untreated control in the repleted centers. D_2O (a kind gift of Dr. D. Cherepanow, Moscow) was exchanged for H_2O by suspending the core particles

after the Ca^{2+} depletion procedure at a final concentration of 95% D_2O.

Flash spectrophotometry was performed with the setups built for nanosecond resolution at 827 nm and for measurements in the UV/Vis region as specified in [16,17] with a frequency-doubled, Q-switched Nd-YAG laser (FWHM 2 ns) as flash excitation source. Absorption transients were digitized, averaged, and stored on a MicroVax. The calibration of transients in terms of $\Delta\varepsilon$ was performed on the basis of 85 chlorophyll molecules per PS II in the core particles [24]. Spectra were not corrected for small flattening effects. DCBQ and hexacyanoferrate(III) served as artificial electron acceptors (see figure legends).

Proton release was recorded with the pH indicating dyes (30 μM) bromocresol purple (pH 6) at 575 nm and phenol red (pH 7.5) at 559 nm [24]. At these wavelengths transients in the absence of dye were negligible as checked by measurements with 50 mM of Mes buffer (not shown) which suppressed all pH transients. For the proton release measurements the buffers were omitted in all media of the Ca^{2+} depletion/repletion procedures. The concentrations of citrate and EDTA were reduced tenfold to keep the buffering capacity of the medium sufficiently low.

3. Results

3.1. The rate of electron transfer $Y_Z \rightarrow P_{680}^+$ in Ca^{2+}-depleted PS II core particles

Fig. 1 shows flash-induced absorption transients at 827 nm in Ca^{2+}-depleted PS II core particles and in controls, namely Ca^{2+}-repleted material. The decay of these transients reflects the electron transfer to P_{680}^+. It was fast in controls (Fig. 1, left column) and about 1000-fold slower in Ca^{2+}-depleted material (note different time bars in Fig. 1). In the Ca^{2+}-repleted control and at pH 6 (upper row, left), the greater portion (75%) of P_{680}^+ decayed with a half-time of 17 ns on flash #1 (Table 1) and multiphasically with half-times of 17, 50, and 280 ns on flash #4. These half-times are typical for the reduction of P_{680}^+ by Y_Z in oxygen-evolving core particles of the used type [19,28]. At least 75% of PS II were apparently repleted by the addition of 20 mM Ca^{2+}.

In Ca^{2+}-depleted centers and at pH 6 (upper row, middle), the 'fast' component of a multiexponential fit was about 1000 times slower than in fully functional centers with a half-time of 40 μs upon flash #1
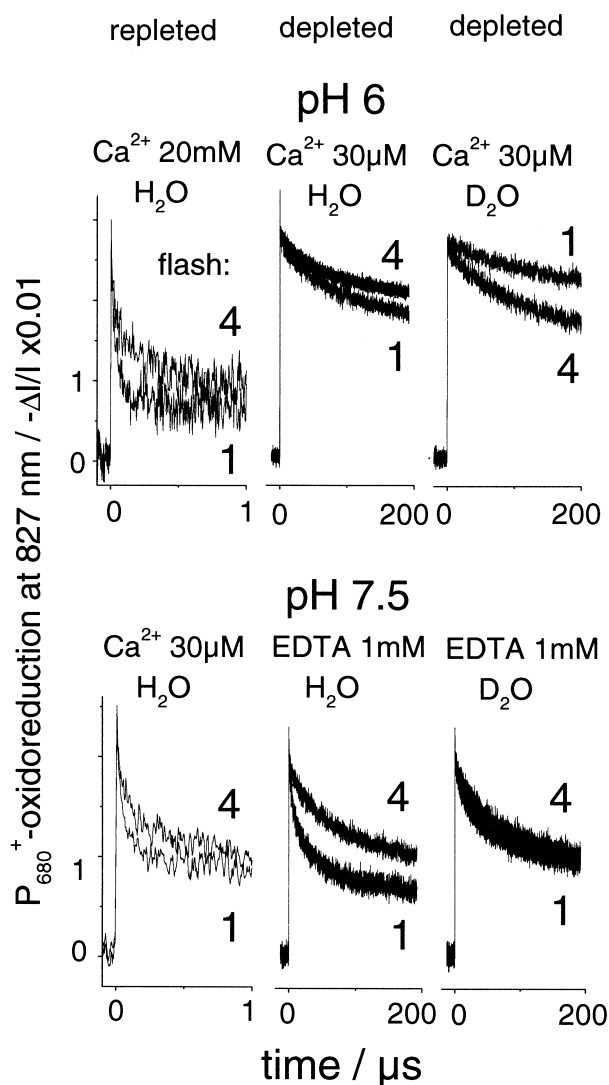

Fig. 1. Absorption transients at 827 nm which specifically indicate the oxidation (rise) and the reduction (decay) of P_{680}. The response to flashes #1 and #4 given to dark-adapted PS II core particles is documented. Measurements were performed at pH 6 (upper traces) and pH 7.5 (lower traces) with PS II core particles depleted of Ca^{2+}. The addition of $CaCl_2$ and EDTA and the substitution of D_2O (95% pure) for H_2O is indicated where applicable. The chlorophyll concentration was 50 μM. DCBQ, 0.5 mM, and hexacyanoferrate(III) 1 mM served as electron acceptors. The optical pathlength was 5 cm, 4–8 transients were averaged for signal-to-noise improvement. The time resolution was 4 ns per address (repleted centers) and 20 ns (depleted material). Note different scales of the time axes.

Table 1
Half-times of electron transfer $Y_Z \rightarrow P_{680}^+$ on flash number 1 in dark-adapted, Ca^{2+}-depleted PS II core particles and in controls

	pH 6.0			pH 7.5		
	Ca^{2+}-repleted	Ca^{2+}-depleted	Ca^{2+}-depleted	Ca^{2+}-repleted	Ca^{2+}-depleted	Ca^{2+}-depleted
Conditions	Ca^{2+} 20 mM	Ca^{2+} 30 µM	Ca^{2+} 30 µM	Ca^{2+} 30 µM	EDTA 1 mM	EDTA 1 mM
Solvent	H_2O	H_2O	D_2O	H_2O	H_2O	D_2O
Half-time of ET $Y_Z \rightarrow P_{680}^+$	17 ns 75%	40 µs 25% (10 µs 65%)	100 µs 20% (25 µs 55%)	17 ns 50% 7 µs 50%	7 µs 20% (0.7 µs 60%)	15 µs 30% (0.9 µs 60%)

ET, electron transfer; figures in parentheses were taken from [16] and represent Mn-depleted centers at the respective pH.

(Table 1). Its relative extent was decreased on flash #4 and again under excitation with repetitive flashes (at 1 Hz, data not shown). In order to check whether it was attributable to forward electron transfer from Y_Z or to the recombination of P_{680}^+ with Q_A^-, we replaced H_2O by D_2O (upper row, right). Only the 'fast' component revealed a kinetic H/D-isotope effect of 2.5 whereas the remainder decayed with the same averaged half-time of ~ 500 µs both in H_2O and D_2O. The long half-life and the lack of a kinetic isotope effect qualify the slower phases as charge pair

Fig. 2. The relative extents of the microsecond components of P_{680}^+ reduction (closed symbols) and of oxygen evolution (open symbols) in Ca^{2+}-depleted PS II core particles as function of the pH under various conditions. The microsecond components were determined from transients at 827 nm under repetitive flash excitation (0.2 Hz, data not shown, compare Fig. 1). Oxygen evolution was measured with a Clark-type electrode under continuous white light illumination (10 µM chlorophyll, 0.5 mM DCBQ, 0.5 mM hexacyanoferrate(III)). The media contained 20 mM NaCl, 0.03% βDM (w/v), 20 mM BisTris (pH < 7) or tricine (pH > 6.5). ●,○, Ca^{2+} 30 µM; ■,□, EDTA 1 mM; ▲,△, Ca^{2+} 20 mM. Ca^{2+} was provided as $CaCl_2$. O_2 evolution with 20 mM Ca^{2+} (△) at pH 6 was ~ 1200 mg O_2/ mol chl h. The slight decay at pH 7.6 was due to centers which probably have lost Mn [16]. The smooth curve was calculated with a pK of 7.

recombination. This assignment was corroborated by recording transients at 320 nm which were due to $Q_A \rightarrow Q_A^-$ (here not shown, but see [16,29,30]). We attributed the 40 µs (H_2O) and 100 µs (D_2O) components to the reduction of P_{680}^+ by Y_Z, proper.

At pH 7.5 (Fig. 1, lower row), the conditions for Ca^{2+} depletion and repletion differed from those observed at pH 6. About 50% of all centers were already repleted at Ca^{2+} concentrations as low as 30 µM $CaCl_2$. This was apparent from the reappearance at large extent of the 17-ns phase. Only 20% of P_{680}^+ were reduced about 1000 times more slowly with $t_{1/2} = 7$ µs (Table 1). At pH 7.5 the depletion of PS II from Ca^{2+} required the addition of 1 mM EDTA at pH 3.5 (before the pH was elevated to 7.5). Only then the 7-µs component became dominant on flash #1 (Fig. 1, lower row, middle). In D_2O (Fig. 1, right) the fastest component of P_{680}^+ reduction on flash #1 was 15 µs. Again, we interpreted the 'fast' components with half-times of 7 µs (H_2O) and 15 µs (D_2O) as indicative for the reduction of P_{680}^+ by Y_Z. It proceeded more slowly than in Mn-depleted PS II at the same pH (Table 1 shows the latter half-times for comparison, in parenthesis [16]).
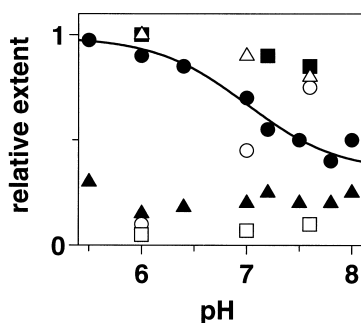
3.2. The pH-dependent affinity for Ca^{2+}-rebinding to Ca^{2+}-depleted PS II core particles

The reported affinities of Ca^{2+} for the reconstitution of oxygen evolution by adding Ca^{2+} to Ca^{2+}-depleted PS II vary by orders of magnitude in the literature (see [1] for a review). Fig. 2 gives a possible clue to this variance. It describes the relative extents of oxygen evolution (observed under continuous light) and of the microsecond component of the reduction of P_{680}^+ by Y_Z (observed under flashing light)

as function of the pH. The ability to evolve oxygen (open symbols) and the appearance of the microsecond component (solid symbols) complement each other. In completely Ca^{2+}-depleted material, i.e., when EDTA was added after the low pH/citrate-treatment but before the pH was elevated, oxygen evolution (open squares) was abolished and P_{680}^+ reduced in μs (closed squares. In controls, i.e., without EDTA and with 20 mM Ca^{2+} present, oxygen evolution was high (open triangles), and the μs-component was converted into the ns-component of intact centers. Unlike the effects of Mn depletion those of Ca^{2+} depletion were largely reversible. The remaining relative extent of the μs-component was only about 20% after Ca^{2+} repletion (closed triangles). It was likely attributable to centers which had lost both Ca^{2+} and Mn. In both cases the behavior showed little pH-dependence in the range from 5.5 to 8. If EDTA was absent and only 30 μM Ca^{2+} was added, oxygen evolution and the μs-component titrated with a pK of about 7, with the former (open circles) increasing and the latter decreasing (closed circles) above pH 7. Apparently, a low affinity Ca^{2+}-binding site with $K_m \gg 30$ μM which prevailed at pH < 7 was replaced by a high affinity site with $K_m \leq 30$ μM which was dominant at alkaline pH (see also [31,32]). Here, the apparent pK of this transition was 7 (see the line in Fig. 2).

3.3. The spectral properties of Y_Z in Ca^{2+}-depleted PS II

Whereas absorption transients at 827 nm are directly attributable to P_{680}, those at 297 nm reflect its electron donors, namely Y_Z and Mn_4X. The contri-
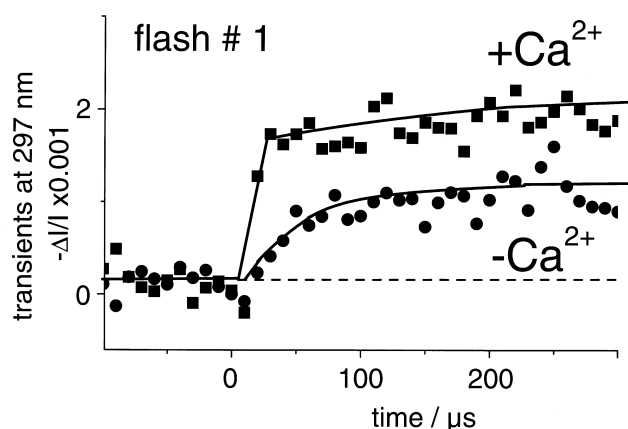

Fig. 3. UV absorption transients at 297 nm on flash #1 given to dark-adapted PS II core particles. The pH was 6. Circles, Ca^{2+}-depleted material; squares, Ca^{2+}-repleted centers. 10 μM chlorophyll, 100 μM DCBQ; optical pathlength 1 cm; 30 transients averaged; time resolution 10 μs per address.

butions of Q_A and P_{680} to this wavelength are small [33]. Fig. 3 shows transients at 297 nm obtained on the first flash in dark-adapted core particles at pH 6. Oxygen-evolving controls revealed the known (here unresolved) rapid rise (attributable to the oxidation of Y_Z by P_{680}^+ in nanoseconds) which was followed by a smaller more slowly rising phase. It reflected the oxidation of Mn by Y_Z^{ox} during the transition $S_1 \Rightarrow S_2$ [19]. This behavior was altered in Ca^{2+}-depleted material. There was only the 40 μs rise present as also apparent in transients at 827 nm (see Table 1, pH 6) which was attributable to the oxidation of Y_Z. It was thus likely that electron transfer stopped at Y_Z^{ox} in the Ca^{2+}-depleted centers already on the first flash.

Did Y_D contribute to the reduction of P_{680}^+? We repeated the measurements at 297 nm but now with material which was subjected to 10 preflashes (in
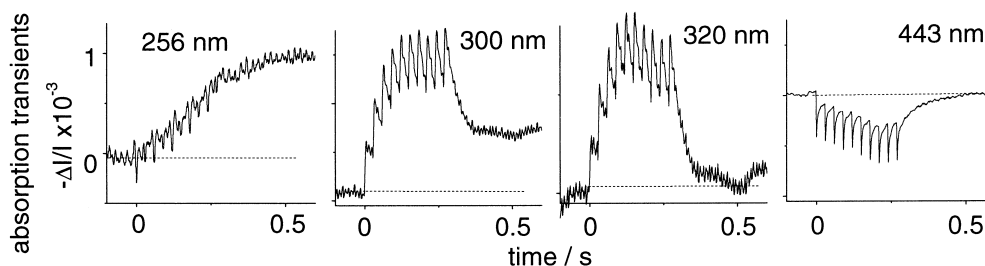

Fig. 4. Absorption transients at various wavelengths induced by ten saturating flashes given to dark-adapted, Ca^{2+}-depleted PS II core particles. The pH was 6. 8 μM chlorophyll, 100 μM DCBQ; 10–30 transients averaged; time resolution 1 ms per address. The spacing between flashes was 30 ms. The measuring wavelength was set by a monochromator which was calibrated against narrow interference filters.

order to preoxidize any Y_D) and thereafter dark-adapted for 15 min. The first flash after this treatment induced essentially the same transients both in the Ca^{2+}-depleted and -repleted centers as obtained without preflashing (data not shown). Furthermore, the difference spectrum of Y_Z in Ca^{2+}-depleted centers was red shifted with respect to the one of Y_D (see below and [36]) and Y_Z^{ox} caused no electrochromic effect as also opposed to Y_D^{ox} [36,37]. It was thus unlikely that Y_D contributed to the observed UV transients. This notion was corroborated by litera-
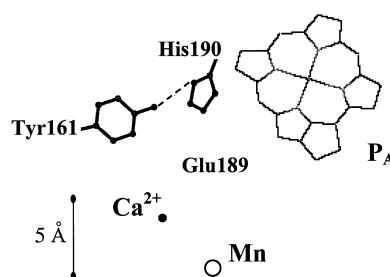
Scheme 1. Tentative locations of cofactors at the catalytic site of water oxidation viewed from Q_A. The triangular placement of Mn, Y_Z, and one of the chlorophylls of P_{680}, P_A, is similar to the one proposed in [8]. The location of Glu189 (E189) and His190 is as in [17]. The particular Mn-atom out of the Mn_4-cluster which receives the electron hole upon $S_1 \Rightarrow S_2$ is symbolized by a circle. We refrained from assigning the other three Mn atoms out of several proposed structures of the Mn_4-cluster [67]. Hydrogen bonding between Y_Z and His190 is shown as a dashed line. Ca^{2+} (dot) was placed at 5.5 Å from Y_Z and at 4 Å from Mn_4.

ture data that both, the reduction of Y_Z^{ox} by Y_D [34]) and of P_{680}^+ by Y_D ([35] and references therein) were much slower (half-time$\geq$1 ms) than by their normal reductants Mn_4X and Y_Z, and that the level of the dark-stable radical, Y_D^{ox}, was found in EPR experiments to be close to 100% and essentially unchanged in PS II that was Ca^{2+}-depleted by the low pH/citrate treatment [27].

To record the difference spectrum of $Y_Z \to Y_Z^{ox}$, Ca^{2+}-depleted PS II was excited with a series of ten flashes (spacing 30 ms). Fig. 4 shows raw absorption transients at four wavelengths as obtained at pH 6. The decay which was apparent after the firing of the last flash was attributable to the oxidation of Q_A^- by DCBQ and to the reduction of P_{680}^+. The remaining more stable component reflected the oxidation of the donor side of PS II with minor contributions of $Q_A \to Q_A^-$ and $P_{680} \to P_{680}^+$ (see also [38]). Its total extent (at 0.5 s after flash #1) as function of the wavelength was plotted in Fig. 5A (pH 6, dashed line). The magnitude of the small contribution of $Q_A \to Q_A^-$ was quantified at 320 nm and the electrochromic band shift of pheophytin *a* in response to Q_A^- at 550 nm as previously [17]. The contribution of $P_{680} \to P_{680}^+$ was determined at 430 nm [17]. The calculated difference spectrum of these contributions is shown in Fig. 5A as a dotted line. It was subtracted from the raw transients. The resulting corrected dif-
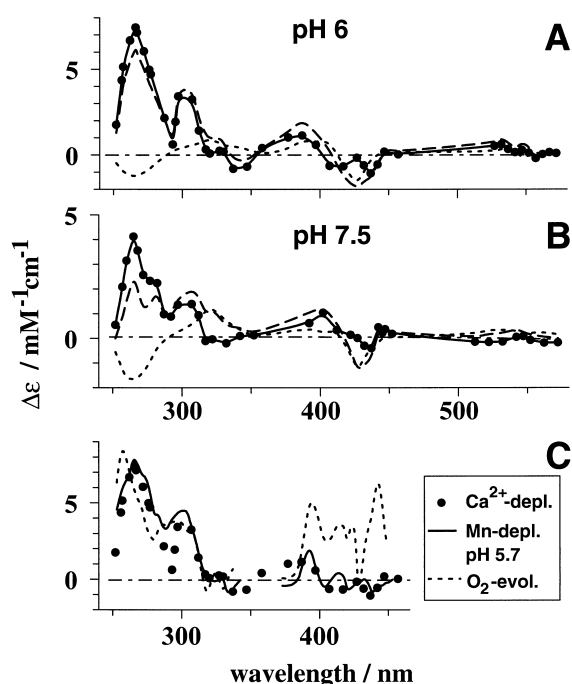
Fig. 5. Optical absorption difference spectra in Ca^{2+}-depleted PS II core particles and in controls. The spectra represent the average over two measurements. The extents were reproducible within one unit of the ordinate scale. (A) The raw spectrum at pH 6 (dashed line) was obtained from the extents of absorption transients at 100 ms after the last flash of a series of ten flashes (see sample documents in Fig. 4). (B) The raw spectrum at pH 7.5 (dashed line) was obtained from the extents of absorption transients at 30 ms after the first flash (data not shown). The contributions of $Q_A \to Q_A^-$ and $P_{680} \to P_{680}^+$ (dotted lines in A and B) were determined as outlined in the text (see also [17]). Their subtraction from the raw spectra yielded the corrected difference spectra of $Y_Z^{ox} - Y_Z$. They are shown in A and B by solid lines/circles. (C) Comparison of the averaged (after normalization at 260 nm) difference spectrum $Y_Z^{ox} - Y_Z$ from Ca^{2+}-depleted PS II (circles) with the respective spectra from control PS II (dotted line) and from Mn-depleted PS II at pH 5.7 (solid line, replotted from [17]).

ference spectrum of the donor side was plotted point-by-point in Fig. 5A (closed circles).

At pH 7.5 the yield of the forward reaction was higher than at pH 6 (Table 1). Fig. 5B (dashed line) shows the extents of transients that were obtained at 30 ms after the first flash given to dark-adapted, Ca^{2+}-depleted PS II core particles. Again, the contributions of $Q_A \rightarrow Q_A^-$ and $P_{680} \rightarrow P_{680}^+$ to these transients were determined (dotted line) and subtracted. The remaining donor side transients were plotted in Fig. 5B (closed circles).

The shapes and peak positions of the corrected difference spectra at pH 6 and 7.5 in Ca^{2+}-depleted PS II core particles (Fig. 5A,B) were quite similar within error limits. The averaged difference spectrum (shown in Fig. 5C as dots) strongly resembled the spectrum $Y_Z^{ox}-Y_Z$ that was obtained with Mn-depleted PS II at acid pH ([17], see also [78]) (Fig. 5C, solid line). Both difference spectra deviated from the $Y_Z^{ox}-Y_Z$ spectrum in oxygen-evolving centers (Fig. 5C, dotted line), both in the UV (see [39] for a survey of literature spectra) and in the blue (electrochromism in response to the formation of Y_Z^{ox} [40]). Recently, spectra of $Y_Z^{ox}-Y_Z$ from Mn-depleted PS II core particles from *Synechocystis* have been reported by Diner et al. [76]. The spectrum

at pH 9 was different from the one at pH 6.1 which was interpreted as a blue shift at pH 6.1 [76]. The authors have claimed an apparent pK of ~ 8.3 for the shift at variance with our data in Refs [16,17] yielding a pK of ~ 7. We recently repeated the set of experiments in [16] but now with core particles from *Synechocystis* and found a similar pK (6.7–7) as in [16] (A. Hays, M. Hundelt, W. Junge, R. Debus, in preparation). Based on our experience and taking into account that the other group used glycerol in the suspending medium in [76] we expected a lower pK, close to 6, for their conditions (see [16] for a similar pK and [44] for the effect of glycerol). The spectra in [76] have been collected at a pH close to or above this expected pK. The spectral differences may be attributable to pH-dependent contributions from Q_A^- and P_{680}^+ (for the correction for such contributions see [17] and this work). The difference spectrum $P_{680}^+-P_{680}$ is indeed negative between 250 and 280 nm [85]. A contribution of this spectrum is expected to be larger at pH 6.1 than at pH 9. The latter effect may account for the lower magnitude of the UV spectrum around 270 nm at pH 6.1 compared to pH 9 in [76], rather than protonation events at Y_Z.

In Ca^{2+}-depleted PS II the UV-peak in the $Y_Z^{ox}-Y_Z$ spectrum was red shifted by about 10 nm
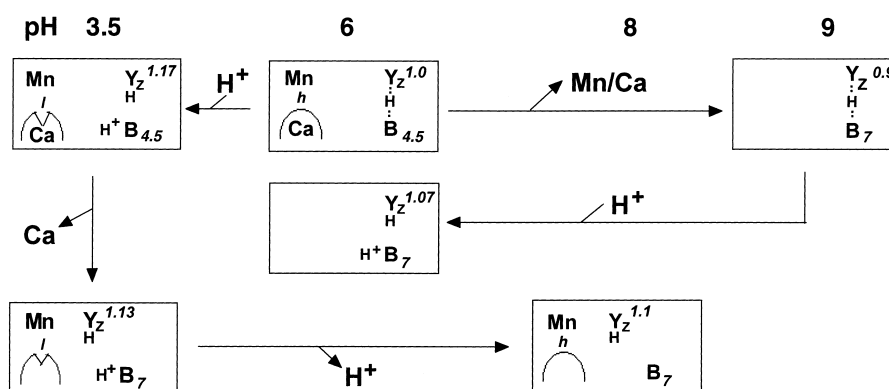
Scheme 2. Hydrogen bonding of Y_Z and its relation to the presence of Mn and Ca^{2+}. Mn denotes the Mn_4-cluster and B the hydrogen-bonded network, one partner of Y_Z being D_1His190. l and h refer to the *l*ow and *h*igh affinities of the Ca^{2+} binding site, and the indices at Y_Z and B stand for the E_m (see below) and the apparent pK, respectively. The arrows symbolize the respective procedures of changing the pH under the various modifications of PS II. The E_m-values of Y_Z have been estimated as follows: In intact PS II the E_m of $Y_Z^{ox}/Y_Z(Y_Z^{\cdot}H^+\cdot B/Y_Z^{(-)\cdot\cdot}H^{(+)\cdot}B$ [17]) was ~ 1 V [62] (compared with ~ 1.1 V of P_{680} [64]). Depletion by Mn and Ca^{2+} lowers it to ~ 0.9 V [63] at alkaline pH. At acid pH, the E_m of the couple $Y_Z^{\cdot}H^+B+H_{bulk}^+/Y_ZH$ H^+B [17], was higher, 1.07 V (as judged from the $\sim 20\%$ equilibrium proportion of P_{680}^+ [16]). In Ca^{2+}-depleted PS II electron transfer $Y_Z \rightarrow P_{680}^+$ occurred in ~ 25 and $\sim 50\%$ of centers at pH 6 and 7.5, the equilibrium proportions of P_{680}^+ were 75% and 50%, yielding 1.13 V (protonated) and 1.1 V (deprotonated). The proton on H^+B thus contributed only ~ 30 mV to the E_m of Y_Z, and 140 mV were likely provided by the hydrogen bonding. Combining these results, Ca^{2+}-binding raises the E_m of Y_Z by 40 mV and Mn_4 by 60 mV.

as compared with oxygen-evolving controls. It should be noted that this feature was robust to a farther reaching correction which also accounted for the contribution of the estimated 20% fraction of centers which had lost both Ca^{2+} and Mn.

In oxygen-evolving centers, large absorption transients are observed in the blue region around 430 nm. Their waved signature has been attributed to the local electrochromic response of chlorophyll *a* to the positive charge of Y_Z^{ox} [8,40,41]. Large electrochromic transients have been observed in oxygen-evolving centers and in Mn-depleted ones at alkaline pH but not in Mn-depleted centers at acid pH (see [16] and references therein for a thorough discussion of this phenomenon). In Ca^{2+}-depleted centers these electrochromic transients were also absent (Fig. 5C). Accordingly, the abstraction of an electron from Y_Z positively upcharged the Y_ZB-entity in controls ([16] and this work), but not in Ca^{2+}-depleted PS II.

How large was the fraction of Y_Z^{ox} that was formed in Ca^{2+}-depleted PS II? At pH 7.5 flash #1 induced 50–65% of the extent of the spectrum $Y_Z^{ox}-Y_Z$ found in Mn-depleted centers. This figure was compatible with the relative extent in Ca^{2+}-depleted PS II of the 7 μs-phase of the electron transfer $Y_Z \rightarrow P_{680}^+$ (Table 1). At pH 6 about 90% of this spectrum were observed after ten flashes. On flash #1 (data not shown) the fraction was 20–30%, compatible with the relative magnitude of the 40 μs-component of P_{680}^+ reduction. We conclude that a series of ten flashes almost fully oxidized Y_Z in Ca^{2+}-depleted PS II core particles.

3.4. One proton is released after the oxidation of Y_Z in Ca^{2+}-depleted centers

Proton release from the donor side was recorded with pH-indicating dyes. Fig. 6A shows raw transients that were induced by a series of ten flashes of light in dark-adapted core particles at pH 6 (left) and pH 7.5 (right).

In controls (Fig. 6A, $+Ca^{2+}$) each flash induced the rapid release of about one proton per PS II as known from previous work [24,44]. The transient proton uptake at pH 7.5 and after the first flash was caused by the acceptor side of PS II upon the reduction of the non-heme iron that was preoxidized in the dark by the electron acceptor hexacyanoferra-

te(III) (for details see [42]). At pH 6 this proton uptake was much smaller because the non-heme iron was less oxidized due to its increased midpoint potential at this pH (increase by ~ 60 mV/pH [43]). Contrastingly, in Ca^{2+}-depleted centers (Fig. 6A,
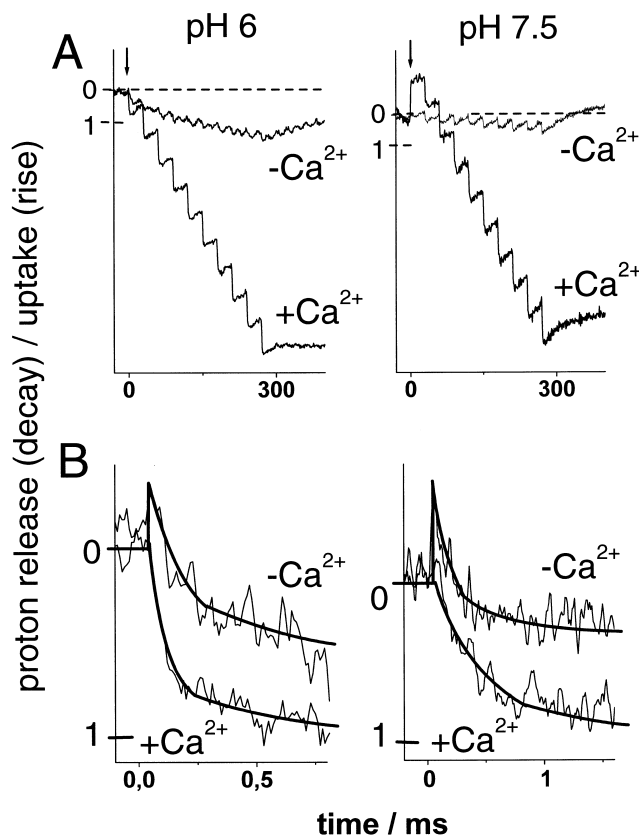

Fig. 6. pH-Indicating absorption transients at pH 6 (left) and pH 7.5 (right) in Ca^{2+}-depleted, dark-adapted PS II core particles and in controls. Bromocresol purple (pH 6, 575 nm) and phenol red (pH 7.5, 559 nm) were used as pH indicators (30 μM). Hexacyanoferrate(III) (100 μM) was used as electron acceptor. (A) Transients induced by 10 saturating flashes spaced by 30 ms. The arrows indicate the first flash. The time resolution was 1 ms per address, 10 transients were averaged. (B) Time-resolved absorption transients on flash one ($-Ca^{2+}$) and flash two ($+Ca^{2+}$) given to dark-adapted PS II core particles. The time resolution was 10 μs per address, 20 transients were averaged. We compared proton release on the second flash in controls with proton uptake/release upon the first flash in Ca^{2+}-depleted material. In the controls the second flash was used because proton release on flash 1 was small [44] and superimposed by proton uptake which complicated the determination of rise-times. Transients were calibrated in terms of protons released per PS II center by setting the average over transients 6–10 from Ca^{2+}-repleted (i.e., oxygen-evolving) material as one proton (see [41]).

$-Ca^{2+}$) proton release was greatly diminished. Its residual small extent on higher flash numbers was probably caused by a fraction of about 20% of centers which were irreversibly depleted of both Ca^{2+} and Mn. At pH 6 the first three flashes led to the accumulated release of about one proton. This proton release was stable within the measuring interval of 0.4 s. At pH 7.5 the net proton release on the first flash was close to zero whereas in the control proton uptake was observed. We interpreted the former behavior as indicating the superimposition of proton uptake upon the reduction of the non-heme iron and of proton release from the donor side (see below).

Rapid proton release from the PS II donor side has been previously observed and attributed to electrostatically induced pK-shifts of peripheral amino acids (see [41,45] for review). This notion has been mainly based on the observation of a hypostoichiometric amount of rapidly released protons over electrons, and on the increase of the rate at acid pH as characteristic for the (fractional) protolysis of acids in contact with water [79]. These deprotonation events were not rate limiting for electron transfer. Furthermore, they did not affect the extents and rates of local electrochromic bandshifts that occurred in the presence of a positive charge on (or near to) Y_Z and Mn_4 [84]. Deviations from this behaviour have been used as markers to unravel the 'chemical' release of protons from the very center, Mn_4XY_Z [2,3,16,41].

Fig. 6B demonstrates time-resolved proton release in controls on flash #2 (see figure legend). At pH 7.5 its half-time was 240 μs and it was diminished to only 50 μs at pH 6, as expected for peripheral events [24]. The rise time of proton release on the first flash in Ca^{2+}-depleted material was about two times slower (pH 6) or faster (pH 7.5) than the one in controls. After the rapid proton uptake upon the reduction of the non-heme iron the release of about 0.5 (pH 6) and 0.9 protons (pH 7.5) with a half-time of about 110 μs was observed. These protons supposedly resulted form the oxidation of Y_Z. There appearance in the medium was delayed when compared with the rise times of electron transfer $Y_Z \rightarrow P_{680}^+$ (Table 1) at both pH values. This behavior may be attributed to the transfer of the proton from Y_Z^{ox} to the bulk along a chain of intervening bases.

4. Discussion

4.1. The oxidation of the donor side in Ca^{2+}-depleted PS II

In active PS II four oxidizing equivalents can be stored on Mn_4XY_Z before oxygen is liberated. After Ca^{2+} depletion the storage capacity is reduced and oxygen evolution is inhibited [9,10]. In this case the highest attainable oxidation state is characterized by the so-called split EPR signal at $g = 2$. Its hyperfine structure has been attributed to the paramagnetic interaction between two components. The chemical identity of the couple is under contention. It has been assigned to Mn and an amino acid radical [46,47], to Mn and the tyrosine radical Y_Z^{ox} [38,48,74,75], and to Y_Z^{ox} and a second organic radical [49,50]. To reduce this ambiguity we studied the UV difference spectrum of the donor side in dark-adapted, Ca^{2+}-depleted PS II. It resembled the known difference spectrum of $Y_Z^{ox} - Y_Z$, which implies that the major oxidized component that is formed in a series of flashes is Y_Z^{ox}. Within noise limits there was no mayor contribution of another component, e.g., from Mn_4X. The supposed second oxidized component according to EPR results is either already present in the dark or it is formed under flashing light with even lower quantum yield than Y_Z^{ox}.

4.2. How does Ca^{2+} act on Y_Z?

The reversible Ca^{2+} depletion of PS II leaves the Mn-cluster in place. Thus, Ca^{2+}-depleted material has been used as a model for the oxygen-evolving system. The observed hydrogen-bond structure of Y_Z in Ca^{2+}-depleted material has been claimed to resemble the one in intact PS II [14,15]. In more recent magnetic resonance work on Ca^{2+}-depleted material, two hydrogen bonds to Y_Z have been postulated [80,81]. However, as the data from the latter materials likely comprise contributions from H/D isotopic exchange not only at Y_Z but also at Mn_4, a fit of the data by two exchangeable hydrogen bonds may be fortuitous [77]. It seems as if conclusive magnetic resonance data, which is relevant for the intact system, on the hydrogen bonding of Y_Z is still lacking. Our data on the electron transfer from the donor side to P_{680}^+, on proton release, and on the

UV/Vis difference spectra do not support the notion that Y_Z is similar in oxygen-evolving and Ca^{2+}-depleted centers. In Ca^{2+}-depleted PS II core particles the normal stepping through the S-transitions is impaired. The reduction of P_{680}^+ is slowed by three orders of magnitude, and the formation of Y_Z^{ox} is coupled with the release of one proton into the bulk. The difference spectrum $Y_Z^{ox}-Y_Z$ is red shifted in the UV and local electrochromic effects are absent. All these properties differ from the ones in oxygen-evolving centers but resemble those observed with Mn-depleted PS II at acid pH [17]. These observations prompted us to interpret the properties of Y_Z in Ca^{2+}-depleted centers in terms of the same model [17]. Its features are as follows: In oxygen-evolving PS II, tyrosine Y_Z is hydrogen-bonded to an acid/base cluster B. Already in its reduced state it behaves as a hydrogen-bonded tyrosinate $Y_Z^{(-)}\cdots H^{(+)}\cdot B$. Only this state of Y_Z allows rapid electron transfer to P_{680}^+ in nanoseconds. In Mn-depleted centers the pK of B is raised from about 4.5 to 7. If B is protonated, as at acid pH, its hydrogen bond(s) with Y_Z are disrupted. The reduction of P_{680}^+ by Y_Z is then blocked unless the excess proton in $Y_Z B$ is released into the bulk. Thereby the electron transfer is slowed by orders of magnitude and, as it is coupled to a protolytic reaction, it shows a much larger H/D-isotope effect than before.

The results on Ca^{2+}-depleted PS II in this work fit into this model. It is conceivable that some effects on Y_Z of Mn depletion are a consequence of the concomitant elimination of Ca^{2+}. One role of Ca^{2+} in intact PS II is probably the tuning of the pK of Y_Z into the acid range to make it ready for hydrogen bonding with B (see [16]).

This view is compatible with results from EPR/ENDOR. The spectrum of the radical Y_Z^{ox} is similar in Ca^{2+}-depleted [49] and in Mn-depleted PS II at pH 5.5 [51,52]. It differs from the one in Mn-depleted material at pH 7.5 [52] which, on the other hand, resembles the one of Y_D^{ox}. The EPR-spectral properties in Mn-depleted PS II at acid pH have been attributed to a protonation event in close vicinity of Y_Z. The spectrum of Y_Z^{ox} obtained by high-field EPR at pH 6 has been attributed to a mixture of strongly and very weakly hydrogen-bonded states [53]. Further magnetic resonance work has been carried out at intermediate pH values [38,81–83].

Whether it fits into the above interpretation remains to be shown.

Studies on the hydrogen bonding of Y_Z as obtained by FTIR have revealed similar features of Y_Z and Y_D in Mn-depleted PS II, of Y_Z in Ca^{2+}-depleted PS II [54], and of TyrH in water [55]. The features of the oxidized species Y_Z^{ox} at pH 6, Y_Z^{ox} in Ca^{2+}-depleted centers, and Tyr^{ox} in water were also similar but differed from those of Y_D^{ox} [54,56]. All of this is compatible with the above view. Data obtained at more alkaline pH [57] are so far conflicting. That the spectroscopic properties of Y_Z reported in [57] differed from the ones found by other authors has been tentatively attributed to the neglect of a contribution of Q_A [54,58].

4.3. A model for the interaction between Mn, Ca^{2+}, and Y_Z at the oxidizing side of PS II

The number of Ca^{2+}-atoms that are necessary for oxygen evolution is under debate: Some authors have found one Ca^{2+} [32,65] whereas others found two ions [26,66]. A Ca^{2+} to Mn-distance of 3.3 Å has been inferred from EXAFS-data by some authors [67], whereas others have denied the presence of Ca^{2+} in the ligand sphere of Mn [68]. Mn-depleted centers apparently do not bind Ca^{2+} to its native site(s) [32,66].

Scheme 1 shows a gross model for the arrangement of cofactors at the oxidizing side of PS II. We placed P_{680}, Y_Z, and the particular Mn-atom which receives the electron hole upon transition $S_1 \Rightarrow S_2$ (see legend to Scheme 1) in a triangle when viewed from Q_A, as previously [8]. The respective center-to-center distances are assumed as $Y_Z-P_{680} \geq 12$ Å ([8] and references therein), and as $Y_Z-Mn = 11.5$ Å. The latter figure is at the upper limit of recent estimates of this distance by EPR/ENDOR [48,69,70,76]. According to model structures of PS II [6,7,17] His190, Glu189, and Asp170 of the D_1 subunit are located close to Y_Z. Y_Z, His190, and Glu189 may form a hydrogen-bonded triade [13,17,20,21,39]. This is one way of how the apparent pK of the $Y_Z B$-couple can be lowered to the observed value of about 4.5. The mutation of Glu189 to Gln apparently decreases the affinity of PS II for Ca^{2+} [71]. Recently, the formation of the 'split EPR signal', which is also observed in Ca^{2+}-

depleted centers (see above), has been reported in the Glu189Gly mutant [72]. These results led us to propose that Glu189 may also form part of a Ca^{2+} binding site. This places Ca^{2+} at about 5–6 Å from Y_Z and at 3–4 Å from Mn (Scheme 1). A single Ca^{2+} ion in this position might account for the low pK of Y_ZB.

Scheme 2 summarizes how the depletion of Mn and Ca^{2+} affects Y_Z. In oxygen-evolving PS II Y_Z is hydrogen-bonded to a network B [17] with an apparent pK of about 4.5. We propose that the respective pK and E_m-values (indices in Scheme 2) are determined by hydrogen bonding and the electrostatic interactions between cofactors. Ca^{2+} depletion likely decreases the midpoint potential [59,60] of the S_2/S_1 couple of Mn_4 (~ 900 mV [61]) which can explain the stabilization of the S_2-state [10] and, in turn, the impairment of oxygen evolution (for an estimation of the individual contributions of the charges on Mn_4, Ca^{2+}, and H^+B to the E_m of Y_Z, see the legend to Scheme 2). Glu189 forms part of a high affinity Ca^{2+} binding site. Tris-wash [73] or the incubation of PS II at alkaline pH [16] induce the double depletion of Mn and Ca^{2+}. This rises the pK of Y_ZB to 7. At pH 9 (Scheme 2) hydrogen bonding to Y_Z is still intact. By lowering the pH to 6, i.e., below the pK of 7 in Mn/Ca^{2+}-depleted centers, Y_ZB is protonated and the hydrogen bonding between Y_Z and B impaired. In the D_1His190Gly mutant of *Synechocystis* both the oxidation of Y_Z and the reduction of Y_Z^{ox} are slowed [20,21] for the same reason. The natural proton acceptor/donator of Y_Z is absent.

Incubation of oxygen-evolving PS II at pH 3.5 also leads to the protonation of Y_ZB and to the loss of the hydrogen bonding interaction, but Mn is retained (Scheme 2). The positive charge of the additional proton on B lowers the normally high affinity for Ca^{2+}. This, in turn, causes the release of Ca^{2+} and the pK of Y_ZB rises to 7. In Ca^{2+}-depleted centers the reformation of the hydrogen bond Y_ZB is impaired even if B is deprotonated at alkaline pH. This may be explained by a structural change brought about by the loss of Ca^{2+} which increases the distance between Y_Z and B (Scheme 2). The loss of the proton on H^+B, however, restores the _h_igh affinity of the Ca^{2+} binding site.

5. Outlook

We compared the properties of the tyrosine Y_Z in Ca^{2+}-depleted PS II core particles with the ones in oxygen-evolving, and in Mn-depleted centers. Ca^{2+} modulates the midpoint potentials of both Mn_4 and Y_Z. In oxygen-evolving PS II, Y_Z is a tyrosinate, hydrogen-bonded to a network B ($Y_Z^{(-)\cdots}H^{(+)\cdot}B$) that includes D1His190. D1Glu189 may be a member of the network and furthermore, may participate in the formation of a Ca^{2+}-binding site. The protonation of Y_ZB lowers the normally high affinity for Ca^{2+}-binding. Vice-versa, the loss of Ca^{2+} impairs the hydrogen-bonding interaction by a structural change which not only affects the pK of B but might also increase the distance between Y_Z and B.

Acknowledgements

References

[1] R.J. Debus, Biochim. Biophys. Acta 1102 (1992) 269–352.
[2] M. Haumann, W. Drevenstedt, M. Hundelt, W. Junge, Biochim. Biophys. Acta 1273 (1996) 237–250.
[3] M. Hundelt, M. Haumann, W. Junge, Biochim. Biophys. Acta 1321 (1997) 47–60.
[4] G. Renger, Physiol. Plant. 100 (1997) 828–841.
[5] M. Haumann, A.Y. Mulkidjanian, W. Junge, Biochemistry 36 (1997) 9304–9315.
[6] S.V. Ruffle, D. Donnelly, T.L. Blundell, J.H.A. Nugent, Photosynth. Res. 34 (1992) 287–300.
[7] B. Svensson, C. Etchebest, P. Tuffery, P. van Kan, J. Smith, S. Styring, Biochemistry 35 (1996) 14486–14502.
[8] A.Y. Mulkidjanian, D.A. Cherepanov, M. Haumann, W. Junge, Biochemistry 35 (1996) 3093–3107.
[9] A. Boussac, J.L. Zimmermann, A.W. Rutherford, Biochemistry 28 (1989) 8984–8989.
[10] T. Ono, Y. Inoue, in: M. Baltscheffsky (Ed.), Current Re-

search in Photosynthesis, vol. 1, Kluwer Academic, Dordrecht, 1990, pp. 741–744.

[11] G. Renger, H.J. Eckert, M. Völker, Photosynth. Res. 22 (1989) 247–256.

[12] A. Boussac, P. Setif, A.W. Rutherford, Biochemistry 31 (1992) 1224–1234.

[13] A. Krieger, E. Weis, S. Demeter, Biochim. Biophys. Acta 1144 (1993) 411–418.

[14] R.D. Britt, in: D. Ort, C.F. Yocum (Eds.), Oxygenic Photosynthesis: The Light Reactions, Kluwer Academic, Dordrecht, 1996, pp. 137-164.

[15] C.W. Hoganson, G.T. Babcock, Science 277 (1997) 1953–1956.

[16] R. Ahlbrink, M. Haumann, D. Cherepanov, O. Bögershausen, A. Mulkidjanian, W. Junge, Biochemistry 37 (1998) 1131–1142.

[17] M. Haumann, A. Mulkidjanian, W. Junge, Biochemistry 38 (1999) 1258–1267.

[18] H.J. Eckert, G. Renger, FEBS Lett. 236 (1988) 425–431.

[19] M. Haumann, O. Bögershausen, D.A. Cherepanov, R. Ahlbrink, W. Junge, Photosynth. Res. 51 (1997) 193–208.

[20] A.M. Hays, I.R. Vassiliev, J.H. Golbeck, R.J. Debus, Biochemistry 37 (1998) 11352–11365.

[21] F. Mamedov, R.T. Sayre, S. Styring, Biochemistry 37 (1998) 14245–14256.

[22] F. Rappaport, J. Lavergne, Biochemistry 36 (1997) 15294–15302.

[23] K. Shigemori, H. Mino, A. Kawamori, Plant Cell Physiol. 38 (1997) 1007–1011.

[24] O. Bögershausen, W. Junge, Biochim. Biophys. Acta 1230 (1995) 177–185.

[25] P.J. van Leeuwen, M.C. Nieveen, E.J. van de Meent, J.P. Dekker, H.J. van Gorkom, Photosynth. Res. 28 (1991) 149–153.

[26] T. Ono, I. Inoue, FEBS Lett. 227, (2) (1988) 147–152.

[27] T. Ono, Y. Inoue, Biochim. Biophys. Acta 973 (1989) 443–449.

[28] P.J. van Leeuwen, C. Heimann, F.A.M. Kleinherenbrink, H.J. van Gorkom, in: N. Murata (Ed.), Research in Photosynthesis, Kluwer Academic, Dordrecht, 1992, pp. 341–344.

[29] M. Karge, K.D. Irrgang, S. Sellin, R. Feinaeugle, B. Liu, H.J. Eckert, H.J. Eichler, G. Renger, FEBS Lett. 378 (1996) 140–144.

[30] G. Christen, M. Karge, H.J. Eckert, G. Renger, Photosynthetica 33 (1997) 529–539.

[31] A. Krieger, E. Weis, Photosynth. Res. 37 (1993) 117–130.

[32] P. Ädelroth, K. Lindberg, L.E. Andreasson, Biochemistry 34 (1995) 9021–9027.

[33] G.H. Schatz, H.J. van Gorkom, Biochim. Biophys. Acta 810 (1985) 283–294.

[34] A. Boussac, A.L. Etienne, Biochem. Biophys. Res. Commun. 109 (1982) 1200–1205.

[35] C.A. Buser, L.K. Thompson, B.A. Diner, G.W. Brudvig, Biochemistry 29 (1990) 8977–8985.

[36] R.A. Diner, Tang, X.S. Zheng, M. Dismukes, G.C. Force, D.A. Randall, D.W. Britt, R.D. in: P. Mathis (Ed.), Photo-

synthesis: From Light to Biosphere, Kluwer Academic, Dordrecht, 1995, pp. 229–234.

[37] M. Haumann, Thesis, Universiät Osnabrück, Germany, 1996.

[38] N. Lydakis-Simantiris, P. Dorlet, D.F. Ghanotakis, G.T. Babcock, Biochemistry 37 (1998) 6427–6435.

[39] L.P. Candeias, S. Turconi, J.H.A. Nugent, Biochim. Biophys. Acta 1363 (1998) 1–5.

[40] F. Rappaport, M. Blanchard-Desce, J. Lavergne, Biochim. Biophys. Acta 1184 (1994) 178–192.

[41] M. Haumann, W. Junge, in: D. Ort, C.F. Yocum (Eds.), Oxygenic Photosynthesis: The Light Reactions, Kluwer Academic, Dordrecht, 1996, pp. 165–192.

[42] O. Bögershausen, W. Junge, in: P. Mathis (Ed.), Photosynthesis: From Light to Biosphere, Kluwer Academic, Dordrecht, 1995, pp. 263–266.

[43] V. Petrouleas, B.A. Diner, Biochim. Biophys. Acta 849 (1986) 264–275.

[44] M. Haumann, M. Hundelt, P. Jahns, S. Chroni, O. Bögershausen, D. Ghanotakis, W. Junge, FEBS Lett. 410 (1997) 243–248.

[45] J. Lavergne, W. Junge, Photosynth. Res. 38 (1993) 279–296.

[46] A. Boussac, J.L. Zimmermann, A.W. Rutherford, J. Lavergne, Nature 347 (1990) 303–306.

[47] J. Tso, M. Sivaraja, J.S. Philo, C.G. Dismukes, Biochemistry 30, (19) (1991) 4740–4747.

[48] J.M. Peloquin, K.A. Campbell, R.D. Britt, J. Am. Chem. Soc. 120 (1998) 6840–6841.

[49] Y. Kodera, H. Hara, A.V. Astashkin, A. Kawamori, T. Ono, Biochim. Biophys. Acta 1232 (1995) 43–51.

[50] A.V. Astashkin, H. Mino, A. Kawamori, T.A. Ono, Chem. Phys. Lett. 272 (1997) 506–516.

[51] H. Mino, A.V. Astashkin, A. Kawamori, T.-A. Ono, Y. Inoue, in: P. Mathis (Ed.), Photosynthesis: From Light to Biosphere, Kluwer Academic, Dordrecht, 1995, pp. 559–562.

[52] H. Mino, A.V. Astashkin, A. Kawamori, Spectrochim. Acta 53A (1997) 1465–1483.

[53] S. Un, X.S. Tang, B.A. Diner, Biochemistry 35 (1996) 679–684.

[54] C. Berthomieu, R. Hienerwadel, A. Boussac, J. Breton, B.A. Diner, Biochemistry 37 (1998) 10547–10554.

[55] R. Hienerwadel, A. Boussac, J. Breton, B.A. Diner, C. Berthomieu, Biochemistry 36 (1997) 14712–14723.

[56] R. Hienerwadel, Boussac, A. Breton, J. Berthomieu, C. in: P. Mathis (Ed.), Photosynthesis: From Light to Biosphere, Kluwer Academic, Dordrecht, 1995, pp. 747–750.

[57] S. Kim, B.A. Barry, Biophys. J. 74 (1998) 2588–2600.

[58] H. Zhang, M.R. Razeghifard, G. Fischer, T. Wydrzynski, Biochemistry 36 (1997) 11762–11768.

[59] T. Ono, Y. Inoue, Arch. Biochem. Biophys. 275, (2) (1989) 440–448.

[60] P. van Vliet, A. Boussac, A.W. Rutherford, Biochemistry 33 (1994) 12998–13004.

[61] I. Vass, S. Styring, Biochemistry 30 (1991) 830–839.

[62] J.G. Metz, P.J. Nixon, M. Rögner, G.W. Brudvig, B.A. Diner, Biochemistry 28 (1989) 6960–6969.

[63] C.T. Yerkes, G.T. Babcock, A.R. Crofts, FEBS Lett. 158, (2) (1983) 359–363.

[64] V.V. Klimov, S.I. Allakhverdiev, S. Demeter, A.A. Krasnovskii, Dokl. Akad. Nauk SSSR 249 (1979) 227–230.

[65] J.R. Shen, K. Satoh, S. Katoh, Biochim. Biophys. Acta 936 (1988) 386–394.

[66] G.N. Grove, G.W. Brudvig, Biochemistry 37 (1998) 1532–1539.

[67] V.K. Yachandra, K. Sauer, M.P. Klein, Chem. Rev. 96 (1996) 2927–2950.

[68] J.E. Penner-Hahn, Structure and Bonding (1998) 1–36.

[69] H. Hara, A. Kawamori, A.V. Astashkin, T. Ono, Biochim. Biophys. Acta 1276 (1996) 140–146.

[70] V.A. Szalai, H. Kühne, K.V. Lakshmi, G.R. Eaton, S.S. Eaton, G.W. Brudvig, Biophys. J. 74, (2) (1998) A75.

[71] H.A. Chu, A.P. Nguyen, R.J. Debus, Biochemistry 34 (1995) 5839–5858.

[72] R.J. Debus, Campbell, K.A. Pham, D.P. Hays, A.M.A. Peloquin, J.M. Britt, R.D. in: G. Garab (Ed.), Photosynthesis: Mechanisms and Effects, 1998, in press.

[73] G.T. Babcock, K. Sauer, Biochim. Biophys. Acta 325 (1973) 504–519.

[74] B.J. Hallahan, J.H.A. Nugent, J.T. Warden, M.C.W. Evans, Biochemistry 31 (1992) 4562–4573.

[75] D.J. MacLachlan, J.H.A. Nugent, M.C.W. Evans, Biochemisty 32 (1993) 9772–9780.

[76] D.J. MacLachlan, D.J. MacLachlan, J.H.A. Nugent, J.T. Warden, M.C.W. Evans, Biochim. Biophys. Acta 1188 (1994) 325–334.

[77] B.A. Diner, D.A. Force, D.W. Randall, R.D. Britt, Biochemistry 37 (1998) 17931–17943.

[78] J.P. Dekker, H.J. van Gorkom, M. Brok, L. Ouwehand, Biochim. Biophys. Acta 764 (1984) 301–309.

[79] M. Eigen, Angew. Chem. 12 (1963) 489–588.

[80] D.A. Force, D.W. Randall, R.D. Britt, Biochemistry 33 (1998) 12062–12070.

[81] C. Tommos, J. McCracken, S. Styring, G.T. Babcock, J. Am. Chem. Soc. 120 (1998) 10441–10452.

[82] X.-S. Tang, M. Zheng, D.A. Chisholm, C. Dismukes, B.A. Diner, Biochemistry 35 (1996) 1475–1484.

[83] C. Tommos, X.-S. Tang, K. Warncke, C.W. Hoganson, S. Styring, J. McCracken, B.A. Diner, G.T. Babcock, J. Am. Chem. Soc. 117 (1995) 10325–10335.

[84] M. Haumann, O. Bögershausen, W. Junge, FEBS lett. 355 (1994) 101–105.

[85] S. Gerken, J.P. Dekker, E. Schlodder, H.T. Witt, Biochim. Biophys. Acta 977 (1989) 52–61.